Test MM-PB/SA on True Conformational Ensembles of Protein−Ligand Complexes

Yan Li, Zhihai Liu, and Renxiao Wang*

State Key Laboratory of Bioorganic Chemistry, Shanghai Institute of Organic Chemistry, Chinese Academy of Science, 345 Lingling Road, Shanghai 200032, People's Republic of China

Received January 25, 2010

The molecular mechanics Poisson−Boltzmann surface area (MM-PB/SA) method has been popular for computing protein−ligand binding free energies in recent years. All previous evaluations of the MM-PB/SA method are based upon computer-generated conformational ensembles, which may be affected by the defective computational methods used for preparing these conformational ensembles. In an attempt to reach more convincing conclusions, we have evaluated the MM-PB/SA method on a set of 24 diverse protein−ligand complexes, each of which has a set of conformations derived from NMR spectroscopy. Our results indicate that both MM-PB/SA and molecular mechanics generalized Born surface area (MM-GB/SA) are able to produce a modest correlation between their results and the experimentally measured binding free energies on our test set. In particular, both MM-PB/SA and MM-GB/SA produced better results by using a representative structure ($R = 0.72-0.79$) rather than averaging over the conformational ensemble of each given complex ($R = 0.61-0.74$). A head-to-head comparison with four selected scoring functions (X-Score, PLP, ChemScore, and DrugScore) on the same test set reveals that MM-PB/SA and MM-GB/SA results are marginally better than those produced by scoring funcitons, supporting the value of the MM-PB/SA method. Nevertheless, scoring functions are still more cost-effective options, especially for high-throughput tasks.

INTRODUCTION

Prediction of binding free energy is one of the key issues in molecular recognition studies. It has many important applications, such as structure-based drug design. A whole spectrum of computational methods have been developed for this purpose, from expensive first-principle-based methods, e.g., free energy perturbation (FEP) and thermodynamic integration (TI) methods,[1,2] to fast scoring functions.[3,4] The molecular mechanics Poisson−Boltzmann surface area (MM-PB/SA) method was originally developed by Kollman and co-workers.[5] It assumes that the overall binding free energy can be calculated by combining molecular mechanics (MM) energies and a continuum solvation model (PB/SA or generalized Born surface area, GB/SA). The MM-PB/SA method can be considered as an end-point simplification of the first-principle-based methods, and it has been popular for computing protein−ligand binding free energies in recent years.[6−12] Our literature survey using the ISI Web of Knowledge indicates that since the 2000s, a total of 30−50 articles were published annually about using MM-PB/SA for binding free energy calculation. An objective evaluation of this method is thus important for its appropriate applications.

The principles of the MM-PB/SA method can be summarized as following:[5]

$$\Delta G_{\text{bind}} = G_{\text{complex}} - (G_{\text{protein}} + G_{\text{ligand}}) \quad (1)$$

$$G = H_{\text{gas}} - TS_{\text{config}} + G_{\text{sol}} \quad (2)$$

$$H_{\text{gas}} \approx E_{\text{gas}} = E_{\text{bond}} + E_{\text{angle}} + E_{\text{torsion}} + E_{\text{vdw}} + E_{\text{ele}} \quad (3)$$

$$G_{\text{sol}} = G_{\text{elec}} + G_{\text{SA}} \quad (4)$$

In eq 1, G_{protein}, G_{ligand}, and G_{complex} are the Gibbs free energies of the protein, the ligand, and the protein−ligand complex, respectively. Each of them is calculated with eq 2 by summing up an enthalpy in gas phase (H_{gas}), a solvation free energy (G_{sol}), and a configurational entropy (S_{config}). H_{gas} can be computed by a standard force field, as eq 3, while S_{config} is normally derived from normal model analysis. G_{sol} is further decomposed into an electrostatic (G_{elec}) and a nonpolar (G_{SA}) term, as eq 4. G_{elec} can be computed using either a Poisson−Boltzmann (PB) model or a generalized Born (GB) model. The nonpolar term (G_{SA}) is assumed to be proportional to the solvent accessible surface area (SASA) of a solute molecule by an empirical relationship:

$$G_{\text{SA}} = \gamma \times \text{SASA} + b \quad (5)$$

As an essential characteristic of regular MM-PB/SA computations, a conformational ensemble of the given complex structure is required, which can be prepared through a molecular dynamics (MD) simulation. The final result is typically the mean value of the outcomes of eq 1 on all sampled conformations. Thus, one would expect that quality of the conformational ensemble used in calculations has a major impact on MM-PB/SA results. Due to the defects in current force fields and solvation models, it is not straightforward to assess the quality of a conformational ensemble

* Corresponding author. E-mail: wangrx@mail.sioc.ac.cn. Telephone: 86-21-54925128.

10.1021/ci100036a
Published on Web 08/09/2010

produced by MD simulation. Consequently, evaluations of MM-PB/SA based on such computer-generated conformational ensembles are associated with uncertainties. Previous studies[13−16] on the MM-PB/SA method were all subject to this problem.

In this study, we attempt to address this problem by testing the MM-PB/SA method on "true" conformational ensembles of protein−ligand complexes. At present, most three-dimensional structures of protein−ligand complexes in the Protein Data Bank (PDB)[17] are resolved through either X-ray crystal diffraction or NMR spectroscopy. In the latter case, NMR measurement can provide a number of short-range interatomic distance and torsion constraints for a given protein−ligand complex. The structural model of the given complex is then optimized typically by restrained molecular dynamic simulations, and the final optimized structural model is required to achieve a maximal agreement with the supplied distance and the torsion constraints. Quality of the final structural models can be assessed by some quantitative criteria, such as the number of restraint violations, root-mean-square (rms) deviations, and *R*-factor.[18] Usually multiple structural models have a comparable level of quality in these terms, and thus sometimes multiple structural models are provided in the structural file deposited in PDB. These structural models thus can be considered as a close analog to the true conformational ensemble of the protein−ligand complex under study. Compared to the conformational ensembles generated by MD simulations, these conformational ensembles derived from NMR spectroscopy provide a more solid basis for the evaluation of the MM-PB/SA method.

We have selected the protein−ligand complexes with multiple NMR-resolved structures from the entire PDBbind database,[19,20] a total of 24 diverse protein−ligand complexes, and used them to test the MM-PB/SA method. Such a test will hopefully provide more convincing conclusions on the performance of MM-PB/SA, since it is based on conformational ensembles with experimental origins. As far as we know, this type of test has not been reported in literature before. The details of our method and results will be given in the following sections.

COMPUTATIONAL METHODS

Compilation of the Test Set. Each protein−ligand complex in our test set needs to have the following features. First, its structure should be available in the PDB.[17] More importantly, multiple structural models should be given, which is only possible among the structures resolved by NMR spectroscopy. Note that some NMR structures in the PDB provide multiple structural models, while the others only provide an "average" structure. Therefore, only the NMR structures in the first category were considered in our study. The multiple structures resolved for a protein−ligand complex are illustrated in Figure 1 as an example. Second, a reliable binding constant (K_a) of this complex has been determined by experiments in order to evaluate the MM-PB/SA method. The PDBbind database,[19,20] which is a systematic collection of the binding affinity data for all sorts of biomolecular complexes in PDB, provides an ideal starting point for selecting the test set used in our study. We searched through the complexes formed between proteins and small-molecule ligands in the entire PDBbind database (version 2008, a total of over 4300 complexes with known binding affinity data) and finally obtained 24 complexes meeting the criteria mentioned above.[21−40]

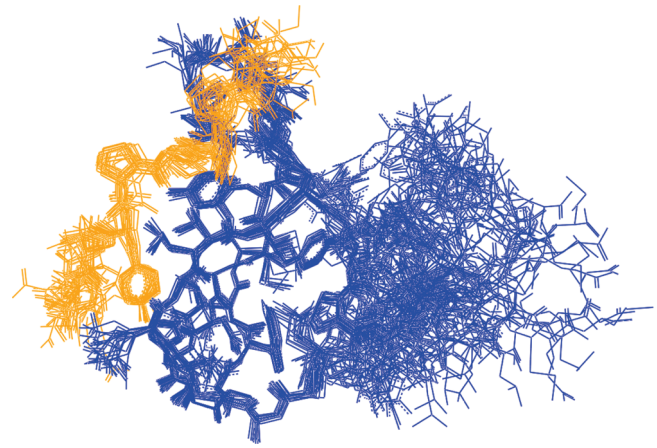

Figure 1. An example of the multiple structural models resolved by NMR spectroscopy (PDB entry 1JMQ, a complex formed by YAP65 and a peptide ligand).

These 24 complexes are formed by 17 different types of protein, and the binding constants of these complexes span over nearly 7 orders of magnitude (Table 1). The standard binding free energy of each protein−ligand complex was calculated as $\Delta G^0_{bind} = RT\ln K_d$, assuming that the dissociation constant (K_d) was measured under standard conditions at a room temperature of 298 K. In addition, we computed the root-mean-squared deviation (rmsd) distribution of the multiple structures of each protein−ligand complex (Table 1). One can see that the average rmsd values of most protein−ligand complexes (23 in 24) here are below 2.8 Å. This level of fluctuation is marginally higher than that of MD-generated conformational ensembles, indicating that the NMR-resolved conformational ensembles considered in our study actually sample a larger conformational space.

Preparation of Complex Structures. Structures of all complexes in our test set were retrieved from the PDB. The multiple structural models of each complex contained in the original PDB data file were separated into a group of single structures for the convenience of subsequent computations. Each complex structure was further split into a protein and ligand molecule. The chemical structure of the ligand molecule was examined manually to assign appropriate atom and bond types. The protein molecule is typically composed of standard amino acid residues so that it was readily acceptable by the AMBER program (version 9)[41] as input.

Each complex structure was then subjected to structural optimization to release possible internal steric repulsions. First, the given protein−ligand complex was soaked in a TIP3P water box with a margin of 10 Å along each dimension. The whole system was neutralized by adding appropriate counterions (Na^+ or Cl^-). After that, structures were allowed to relax through a steepest descent minimization of 100 cycles, followed by a conjugated gradient minimization of 2900 cycles. The convergence criterion (rms gradient) was set to 0.1 kcal/mol·Å. No restraints were applied during energy minimization. These computations were conducted by using the SANDER module in the AMBER program.

Table 1. Basic Information of the 24 Protein−Ligand Complexes in the Test Set

PDB code	K_d (μM)	no. of conformers	ID of the representative conformer[a]	average rmsd (Å)[b]	description (protein + ligand)
1BZF	0.005	22	19	0.94	dihydrofolate reductase/trimetrexate
1DDM	1.7	20	1	2.03	NUMB PTB domain + NAK peptide
2NMB	0.53	14	4	2.50	NUMB PTB domain + phosphotyrosyl peptide
1F40	1	10	1	0.31	FKBP12 + GPI-1046
1FHR	100	20	20	1.63	FHA2 domain of RAD53 + phosphotyrosyl peptide
1IH0	10	30	11	1.68	C-domain of human cardiac troponin C + EMD57033
1LXF	80	30	1	2.31	N-domain of human cardiac troponin C + Bepridil
1J5I	230	44	1	2.02	apo-neocarzinostatin + NCZ
1O5P	0.0001	60	60	0.78	holo-neocarzinostatin + CHR
1JMQ	40	20	1	2.67	YAP65 WW domain + GTPPPPYTVG
1K9Q	700	20	1	2.74	YAP65 WW domain + *N*-(*n*-octyl)-GPPPY-NH_2
1K9R	500	20	1	2.70	YAP65 WW domain + acetyl-PLPPY
1L2Z	203	15	1	1.52	CD2BP2-GYF domain + proline-rich peptide
1P7M	42	25	8	2.04	3-methyladenine DNA glycosylase 1 + ADK
1Q5L	600	15	1	2.25	substrate binding domain of DNAK + NRLLLTG
1XSC	50	25	1	2.02	AP4A hydrolase + ATP
2GTV	7	10	1	2.43	chorismate mutase + TSA
2JMJ	9.1	20	1	2.62	YNG1 protein PHD domain + histone H3
2JOA	1.1	20	1	2.05	serine protease HTRA1 PDZ domain + peptide H1−C1
2JUP	156	10	1	1.73	FBP28WW2 domain + PPLIPPPP
2RLY	270	8	1	1.60	FBP28WW2 domain + PTPPPLPP
2RM0	94	8	1	1.63	FBP28WW2 domain + PPPLIPPPP
2OQS	1.33	30	1	1.34	hDLG/SAP97 PDZ2 domain + HPV-18 E6 peptide
2P0X	0.494	20	1	4.65	abiotic ATP-binding, folding optimized protein + ATP

[a] ID of the "representative conformer" defined by the researchers who resolved this protein−ligand complex structure, which can be found in the corresponding PDB structural file. [b] Average root-mean-squared deviation (rmsd) of all conformers of the given protein−ligand complex. The original structures in the PDB files were used in the computation. For each conformer, its rmsd was computed by using the representative conformer as the reference. Only nonhydrogen atoms were considered in computation.

Both of the structural optimization jobs described above and the subsequent MM-PB/SA computations require appropriate atomic charges assigned on the protein and the ligand. For this purpose, electrostatic potentials of the ligand molecule were obtained through single-point energy calculations at the HF/6-31G(d) level with Gaussian 03.[42] Then, atomic charges on the ligand were derived by using the restrained electrostatic potential (RESP) method[43] implemented in the ANTECHAMBER module of the AMBER program. Amino acid residues on the protein were assigned the template charges in the AMBER FF03 parameter set. All ionizable side chains on amino acid residues were configured in their standard ionization states at pH = 7.0. The AMBER FF03 and GAFF parameter sets were applied to force field computations for proteins and ligands, respectively.

When a molecule undergoes conformational changes, in principle its atomic charges should redistribute as well. Nevertheless, atomic charges are typically fixed in a standard molecular dynamic simulation for technical convenience. In our study, we attempted to explore the effect of charge redistribution on MM-PB/SA results by considering two approaches for assigning atomic charges on ligand molecules. The first approach was to assign the atomic charges derived from a "representative conformation" (as indicated in the original PDB files) to other conformations of the same ligand as well, which will be referred to as "*static charges*" in this article. The second approach was to recompute the atomic charges for each ligand conformation using the methods described in the previous paragraph, which will be referred to as "*dynamic charges*" in this article. In both cases, atomic charges assigned on the protein molecule, i.e., the template charges in the AMBER FF03 parameter set, were still kept fixed.

Binding Free Energy Computation. The basic principles of the MM-PB/SA method have been described in the Introduction Section of this article. All MM-PB/SA computations in our study were conducted by using the AMBER program (version 9).[41] H_{gas} in eq 2 was computed by using the same set of force field parameters for structural optimization described in the previous session. S_{config} in eq 2 was computed through normal-mode analysis with the NMODE module. G_{sol} in eq 4 was computed with the PB/SA model implemented in the PBSA module. The GB/SA model implemented in the same module was also applied to compute G_{sol} to make a comparison. The dielectric constants of solute and solvent were set as 1 and 80, respectively. Default values were adopted for other parameters relevant to the PB/SA or GB/SA model.

Also, the nomenclature used in this article has to be clarified here. As mentioned above, either a PB or GB model may be employed to compute the solvation energy. Thus, we will use "MM-PB/SA" or "MM-GB/SA" wherever it is necessary to differentiate these two options. Otherwise, we will use "the MM-PB/SA method" to represent the general computational routine defined by eqs 1−5. Correlation between the experimental binding free energies and the MM-PB/SA or -GB/SA results was evaluated by the standard least-squares regression analysis.

Sampling Methods. An essential character of the MM-PB/SA method is that the final predicted binding free energy of a given protein−ligand complex is based on the results obtained on a conformational ensemble of the complex structure, which is normally generated by a molecular dynamics simulation in standard MM-PB/SA computations. The default method provided by AMBER, which is the most popular one in practice, is to take the mean value of the computed results on all sampled conformations as the final

Table 2. MM-PB/SA Results Obtained under Different Settings

			MM-PB/SA results obtained on						
			conformational ensembles (method 1)		representative conformations (method 2)	lowest energy conformations (method 3)		lowest binding free energy conformations (method 4)	
PDB code	$-\log K_d$	ΔG_{exp} (kcal/mol)[a]	dynamic charges	static charges	static charges	dynamic charges	static charges	dynamic charges	static charges
1BZF	8.30	−11.32	−28.55	−28.20	−31.07	−33.35	−26.42	−39.50	−49.35
1DDM	5.77	−7.87	7.17	4.53	−1.08	17.44	10.33	−12.80	−25.84
1F40	6.00	−8.18	−10.73	−9.13	−7.52	−7.81	−12.90	−18.68	−19.44
1FHR	4.00	−5.45	−6.30	−8.13	1.35	9.58	20.38	−28.61	−34.06
1IH0	5.00	−6.82	−3.21	−2.18	−1.78	5.97	1.27	−18.35	−12.37
1J5I	3.64	−4.96	8.80	10.09	6.64	5.72	2.01	−8.36	−8.46
1JMQ	4.40	−6.00	0.22	1.17	−0.25	1.55	9.64	−11.92	−14.13
1K9Q	3.15	−4.30	3.63	3.58	5.74	2.89	7.75	−8.67	−4.76
1K9R	3.30	−4.50	7.79	6.56	4.89	17.15	0.57	−4.43	−4.23
1L2Z	3.69	−5.04	−19.35	−17.79	−10.37	−7.48	−13.41	−31.54	−33.36
1LXF	4.10	−5.59	−2.55	−6.91	3.58	3.58	3.58	−19.05	−28.95
1O5P	10.00	−13.64	−13.75	−14.01	−13.30	−9.77	−8.47	−26.16	−30.39
1P7M	4.38	−5.97	3.18	4.52	−11.59	−4.67	−9.26	−19.69	−11.59
1Q5L	3.22	−4.39	−3.43	−8.40	−22.64	−22.64	−22.64	−22.64	−22.64
1XSC	4.30	−5.87	15.42	11.65	6.59	11.72	22.50	−44.45	−30.85
2GTV	5.15	−7.03	−71.26	−74.67	−76.59	−37.46	−44.59	−94.21	−99.85
2JMJ	5.04	−6.87	−11.15	−11.50	−10.96	6.87	9.70	−39.39	−27.71
2JOA	5.96	−8.13	−14.08	−13.87	−11.59	−23.86	−11.64	−26.44	−31.41
2JUP	3.81	−5.19	0.02	2.23	5.09	0.94	1.16	−7.62	−5.56
2NMB	6.28	−8.56	−5.97	−7.55	−10.74	−32.88	−42.44	−32.88	−42.44
2OQS	5.88	−8.01	−19.52	−19.69	−21.61	−26.53	−10.51	−36.49	−43.76
2P0X	6.31	−8.60	−37.36	−34.59	−24.45	−47.61	−24.16	−66.52	−60.51
2RLY	3.57	−4.87	−1.22	2.16	0.94	−5.45	0.76	−9.43	−0.14
2RM0	4.03	−5.49	3.21	4.42	4.53	−1.63	3.36	−2.23	−3.52
correlation coefficient (R)[b]			0.579	0.610	0.721	0.556	0.521	0.465	0.605
standard deviation (SD, kcal/mol)			1.92	1.87	1.63	1.96	2.01	2.09	1.88

[a] The experimental binding free energy is calculated as $\Delta G_{exp} = 2.303RT\log K_d$, $T = 298$ K. [b] All correlation coefficients are calculated after excluding two outliers (PDB entries 1Q5L and 2GTV) which undergo substantial conformational changes upon ligand binding (see Results and Discussion Section).

result. There are of course other possible sampling methods for this purpose. In our study, the binding free energy of each protein−ligand complex in our test set was calculated by using the following four sampling methods, respectively:

(i) The standard sampling method was to sample all conformations and take the mean value as the final result (method 1).

(ii) The final binding free energy was computed based on a "representative conformation" of the given complex (method 2). The representative conformation is specified in the original PDB file by the researchers who resolved the complex structure. It should be emphasized that the other conformations are not necessarily less accurate. In fact, all conformations meet the essential distance and torsion constraints derived from NMR spectroscopy, and they are typically the lowest energy ones selected out of a larger ensemble.

(iii) The final binding free energy was computed based on the conformation with the lowest total energy across the entire conformational ensemble of the given complex (method 3).

(iv) The final binding free energy was the lowest MM-PB/SA binding free energy obtained on a certain conformation across the entire conformational ensemble (method 4).

Thus, except for the first method, the final binding free energies computed by the other three methods are actually based on one single conformation of the given complex.

Scoring Functions. Four scoring functions were also evaluated on the same test set considered in our study to make comparison with MM-PB/SA results, including X-Score,[44] DrugScore^{CSD},[45] PLP,[46,47] and ChemScore.[48,49] These four scoring functions were selected because our recent study[50] suggested that they were the top four in terms of reproducing binding affinity data among a range of popular scoring functions. In this study, X-Score (version 1.3) was acquired directly from its original authors; DrugScore refers to DrugScore^{CSD} (version 0.9), which is publicly accessible at http://pc1664.pharmazie.uni- marburg.de/drugscore/index.php. PLP refers to the PLP1 scoring function implemented in the Discovery Studio software (version 2.1, Accelrys Inc.); and ChemScore refers to the ChemScore scoring function implemented in the SYBYL software (version 7.3, New Tripos Inc.) The same complex structures prepared for MM-PB/SA computation were subjected to these scoring functions where format conversion was conducted when necessary. Correlation between the experimental binding free energies and the binding scores produced by these scoring functions were also evaluated by the standard least-squares regression analysis.

RESULTS AND DISCUSSION

General Performance of MM-PB/SA and MM-GB/SA. Most successful applications of MM-PB/SA reported so far consider a congeneric series of compounds binding with a certain target protein.[6,9,14] The principles of MM-PB/SA, however, does not limit its application to such cases. In our study, MM-PB/SA was tested on a number of protein−ligand complexes formed by various types of proteins and ligands (Table 1). This of course represents a more challenging test, which hopefully can explore the general performance of MM-PB/SA further.

Table 2 gives both the experimentally measured binding free energies (ΔG_{exp}) and the calculated values (ΔG_{cal}) for all 24

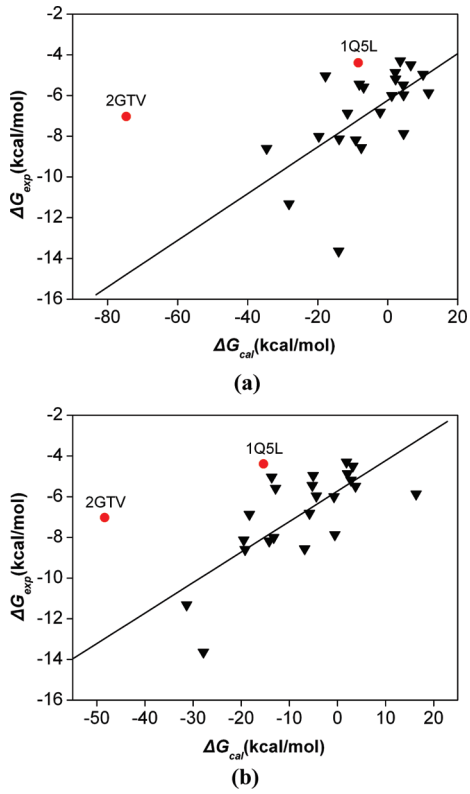

Figure 2. Correlations between the experimental binding free energies (ΔG_{exp}) and the calculated values (ΔG_{cal}) by averaging over conformational ensembles with (a) the MM-PB/SA method: $N = 22$, $R_p = 0.610$, SD = 1.87 kcal/mol and (b) the MM-GB/SA method: $N = 22$, $R_p = 0.743$, SD = 1.58 kcal/mol. PDB entries 1Q5L and 2GTV are not included in correlation analysis, which are indicated on this figure in red solid circles.

complexes in our test set. Our results indicate that there is a modest correlation between the MM-PB/SA results and the experimental binding free energies. If the standard sampling method (method 1) is employed, the Pearson correlation coefficient (R) between these two sets of data is 0.610, and the standard deviation (SD) is 1.87 kcal/mol (Figure 2). Note that two significant outliers (PDB entries 1Q5L and 2GTV) are excluded from the above correlation analysis (Table 2). Still, considering the structural diversity of the remaining 22 complexes, this result is encouraging rather than discouraging.

MM-GB/SA produced better correlations than MM-PB/SA on our test set (Table 3). The Pearson correlation coefficient (R) between the MM-GB/SA results and experimental binding free energies on the same 22 complexes is 0.743, and the standard deviation (SD) is 1.58 kcal/mol under the same condition (Figure 2). In fact, MM-GB/SA results are consistently better than MM-PB/SA results no matter what sampling method is employed. Moreover, MM-GB/SA results are less sensitive to different sampling methods than MM-PB/SA results. The same trend was observed in our previous study of PTP1B inhibitors with the MM-PB/SA method as well.[51] It is also interesting to observe that MM-GB/SA results are also generally associated with smaller fluctuations than MM-PB/SA results on the same set of conformational ensemble of each protein−ligand complex (see the Supporting Information). In other words, MM-GB/SA results are less sensitive to conformational changes than MM-PB/SA results. All these advantages suggest that MM-GB/SA is a more robust option in practice.

Note that the only difference between MM-PB/SA and MM-GB/SA is whether a PB[52,53] or GB model[54] is applied to compute the electrostatic term in solvation energy (eq 4). When used with the dielectric screening algorithm introduced by Still,[55] it has been demonstrated that GB models can produce results with comparable accuracy to PB models on small molecules. Thus, it is interesting to discuss why MM-GB/SA is observed in our study as a more robust method than MM-PB/SA. Assume that a solute molecule has a set of atomic charges on it. In brief, PB models rely on the Poisson equation, which describes the electrostatic potential $\varphi(r)$ generated by this charge distribution $\rho(r)$ in a continuum model of a polarizable solvent with dielectric constant $\varepsilon(r)$:

$$\nabla[\varepsilon(r)\nabla\phi(r)] = -4\pi\rho(r) \tag{6}$$

Electrostatic energies are computed by a finite integration of the solutions to this equation across the space of interest. This space covers the solute molecule itself as well as its surrounding regions. When a solute molecule changes its conformation, both the space of interest and the electrostatic potentials in it will be redefined, which in turn alters the results of the Poisson equation. GB models use analytical expressions based on the Born ion model to approximate the electrostatic potentials of a solute molecule:

$$\Delta G_{GB} = -\frac{1}{2}\left(1 - \frac{1}{\varepsilon}\right)\sum_{i}^{N}\sum_{j}^{N}\frac{q_i q_j}{f_{GB}} \tag{7}$$

As indicated in the above equation, a GB model basically sums up pairwise interactions inside a charge distribution. Thus, GB models are generally faster than PB models. More importantly, when a solute molecule changes its conformation, it is reasonable to expect that the resulting charge redistribution on the solute molecule will not be as significant as the change in the shape and thereby the surrounding regions of the solute molecule. Consequently, GB results are less sensitive to conformational changes. This is probably why MM-GB/SA was observed to produce more converged results in our study.

On the other hand, our results indicate that neither MM-PB/SA nor MM-GB/SA can really reproduce the absolute values of binding free energies (see Tables 2 and 3). The calculated binding free energies are comparable to the experimental data only in a few cases in our test set. Sometimes the calculated binding free energies are even positive. As indicated by eq 2, the MM-PB/SA method decomposes Gibbs free energy into three basic components, an enthalpy term computed by a force field, a solvation energy term computed by a PB/SA or GB/SA model, and a configurational entropy term computed by normal-mode analysis. Historically, these three types of theories were validated separately on some model systems. Thus, one has to be very careful to reconcile them together to reproduce subtle free energy difference even if the theoretical basis of eq 2 is correct. Our opinion is that predicting the absolute values of binding free energies may not be a cherished goal for MM-PB/SA or MM-GB/SA computations. Although some researchers claimed that they had successfully produced absolute binding free energies with the MM-PB/SA method,[56,57] it seems that such results were probably fortuitous. The MM-PB/SA method should be more useful for comparing the

Table 3. MM-GB/SA Results Obtained under Different Settings

			MM-GB/SA results obtained on						
			conformational ensembles (method 1)		representative conformations (method 2)	lowest energy conformations (method 3)		lowest binding free energy conformations (method 4)	
PDB code	$-\log K_d$	ΔG_{exp} (kcal/mol)[a]	dynamic charges	static charges	static charges	dynamic charges	static charges	dynamic charges	static charges
1BZF	8.30	−11.32	−31.71	−31.33	−30.91	−36.38	−29.58	−40.35	−48.89
1DDM	5.77	−7.87	1.81	−0.54	−10.12	10.93	4.70	−12.93	−20.03
1F40	6.00	−8.18	−16.43	−14.19	−12.41	−11.56	−18.94	−27.44	−27.87
1FHR	4.00	−5.45	−2.03	−5.22	17.39	−0.57	0.47	−27.37	−36.35
1IH0	5.00	−6.82	−6.72	−5.82	0.10	−0.57	−4.57	−18.21	−15.36
1J5I	3.64	−4.96	−5.91	−5.06	−4.71	−4.68	−8.54	−23.08	−19.56
1JMQ	4.40	−6.00	−1.35	−0.71	3.37	−1.90	5.98	−11.07	−18.00
1K9Q	3.15	−4.30	1.83	1.89	3.56	1.46	6.50	−9.12	−6.11
1K9R	3.30	−4.50	4.44	3.18	1.35	16.52	0.66	−5.08	−6.66
1L2Z	3.69	−5.04	−15.22	−13.66	−10.61	−4.34	−12.28	−27.88	−26.33
1LXF	4.10	−5.59	−9.05	−12.86	−2.89	−2.89	−2.89	−25.01	−36.86
1O5P	10.00	−13.64	−28.55	−27.85	−31.65	−29.18	−28.10	−38.74	−40.11
1P7M	4.38	−5.97	−5.76	−4.37	−15.40	−13.79	−18.29	−26.44	−18.29
1Q5L	3.22	−4.39	−10.80	−15.36	−24.75	−24.75	−24.75	−24.75	−25.57
1XSC	4.30	−5.87	18.85	16.35	16.66	19.44	25.56	−14.12	−14.30
2GTV	5.15	−7.03	−45.18	−48.35	−58.14	−19.55	−26.69	−58.14	−65.40
2JMJ	5.04	−6.87	−17.68	−18.30	−15.12	−2.17	0.91	−38.60	−33.98
2JOA	5.96	−8.13	−19.21	−19.47	−18.30	−30.26	−18.56	−30.26	−34.67
2JUP	3.81	−5.19	0.97	2.80	4.71	0.97	2.07	−6.23	−5.27
2NMB	6.28	−8.56	−4.19	−6.82	−12.59	−27.37	−39.32	−27.37	−39.32
2OQS	5.88	−8.01	−13.63	−13.25	−17.96	−19.50	−5.97	−28.05	−32.83
2P0X	6.31	−8.60	−24.01	−19.18	−15.33	−35.26	−16.09	−48.21	−41.44
2RLY	3.57	−4.87	−1.21	2.10	1.29	−5.27	−0.04	−8.39	−1.34
2RM0	4.03	−5.49	2.85	3.76	1.69	−1.78	2.56	−2.15	−6.64
correlation coefficient (R)[b]			0.721	0.743	0.788	0.718	0.656	0.665	0.637
standard deviation (SD, kcal/mol)			1.63	1.58	1.45	1.64	1.78	1.76	1.82

[a] The experimental binding free energy is calculated as $\Delta G_{exp} = 2.303RT\log K_d$, $T = 298$K. [b] All correlation coefficients are calculated after excluding two outliers (PDB entries 1Q5L and 2GTV) which undergo substantial conformational changes upon ligand binding (see Results and Discussion Section).

relative binding affinities of a set of protein−ligand complexes, which has been demonstrated repeatedly by other researchers[16] as well as ourselves.[9,51] In addition, the accuracy of the MM-PB/SA method reported in previous studies, if measured by the standard deviations between experimental and computed data, ranges from 1−2 kcal/mol or even higher. It is thus probably not realistic to expect the MM-PB/SA method to correctly interpret small free energy differences. Thus, we believe that the MM-PB/SA method would better be used to distinguish between strong and weak binders. The same statement was also made, for example, by Stahl[13] and Pearlman[14] in their studies.

On Atomic Charge Assignment. Atomic charges are required to compute the electrostatic term in the force field energy (eq 3) and the electrostatic component in the solvation energy (eq 4). Thus, the method for assigning atomic charges also has an influence on the final results of MM-PB/SA computation. In principle, atomic charges on a given molecule will redistribute when its conformation undergoes changes. In a standard MM-PB/SA routine, however, the atomic charges assigned on both protein and ligand are fixed for convenience, although different conformations are considered in computation. An alternative approach is to recalculate the atomic charges on each conformation under consideration. This approach is of course computationally more demanding but may reflect the physics in protein−ligand binding better.

In our study, two approaches for atomic charge assignment, i.e., "static" and "dynamic" charges, have been tested. One can see in Tables 2 and 3 that the calculated binding free energies with "dynamic charges" are different by 3−4 kcal/mol from those with static charges on quite a few protein−ligand complexes in our test set, e.g., PDB entries 1LXF, 1XSC, 1Q5L, and 2RLY. This observation indicates clearly the influence of the atomic charge scheme on MM-PB/SA results. Nevertheless, considering the overall correlation between experimental and calculated data, the dynamic charges approach does not produce better results than those of the standard static charges approach for both MM-PB/SA ($R = 0.579$ vs 0.610) and MM-GB/SA ($R = 0.721$ vs 0.743).

It is somewhat disappointing that adopting dynamic charges has not led to improved results for either MM-PB/SA or MM-GB/SA. We noticed that Ryde et al[15] reported similar results in their application of the MM-PB/SA method to the study of the binding of seven biotin analogues to avidin. In that study, they attempted to recalculate atomic charges at the HF/6-31G(d) level for each MD snapshot of the ligand structure. Interestingly, they also obtained worse results by doing so as compared to the standard static charges approach. Ryde et al attributed this unfavorable result to the technical problems associated with the dynamic charges approach. We basically agree with this point of view. In our study, the dynamic charges approach is applied only to the ligand side, whereas atomic charges on the protein side are still kept fixed. It will require a tremendous amount of computation to apply the same level of theory, i.e., HF/6-31G(d), to the protein side as well. Even if it is fully practical

Table 4. Pearson Correlation Coefficients between Experimentally Measured Binding Free Energies and MM-PB/SA and MM-GB/SA Results under Different Settings[a]

	MM-PB/SA		MM-GB/SA	
sampling methods	with S_{config}[b]	without S_{config}[c]	with S_{config}	without S_{config}
consider conformational ensembles (method 1)	0.610	0.480	0.743	0.603
consider the representative conformations (method 2)	0.721	0.503	0.788	0.673
consider the conformations with the lowest total energy (method 3)	0.521	0.537	0.656	0.678
consider the conformations with the lowest binding free energy (method 4)	0.605	0.379	0.637	0.426

[a] All correlation coefficients are calculated after excluding two outliers (PDB entries 1Q5L and 2GTV). [b] The final computed binding free energies include the configurational entropy term. [c] The final computed binding free energies do not include the configurational entropy term.

at all, one could still argue that charge distribution computed in vacuum is very different from the reality in solvent.

Due to these technical problems, although the dynamic charges approach is conceptually attractive, it seems unnecessary to apply it to MM-PB/SA computations. In fact, assigning appropriate atomic charges is always a major challenge for all force field-based computations. The next generation of force fields may needs to adopt some terms accounting for the polarization effect, such as the study by Queen et al.[58] Before any convincing charge scheme is developed, the standard static charges approach is just acceptable for MM-PB/SA computations.

Configurational Entropy and Protein Flexibility. Another elusive factor in MM-PB/SA computation is the configurational entropy (S_{config} in eq 2). Conceptually, this energetic term is also indispensable in protein−ligand binding free energy. In our study, we computed this energy term for each protein−ligand complex through normal-mode analysis and compared the final results by including and excluding this term. Our results indicate that if excluding S_{config}, the correlations between calculated binding free energies and experimental data become apparently worse for both MM-PB/SA and MM-GB/SA (Table 4). The same trend is actually observed with other sampling methods tested in ours study as well.

Thus, our results clearly support the value of the configurational entropy term in the MM-PB/SA method. Some previous studies on MM-PB/SA actually came to the same conclusion.[9,10] However, those studies were all based on structural models generated by MD simulations, whereas our results are obtained on structural models with experimental basis, which should be more convincing. On the other hand, our results also indicate that the configurational entropy term shows a fairly large variation across the conformational ensemble of each protein−ligand complex. This is of course not desirable for obtaining converged results. Therefore, better methods for estimating S_{config} are still much needed.

Another related issue is conformational flexibility. Our results reveal that the MM-PB/SA method shows obvious limitations on systems with significant flexibility. In our test set, there are two such cases: one is the substrate binding domain of HSP70 (DNAK) in complex with an oligo-peptide (PDB entry 1Q5L), and the other is chorismate mutase in complex with a transition-state analog (PDB entry 2GTV). The overall correlation between the MM-PB/SA or MM-GB/SA results and the experimental data would become much worse if these two cases were considered in correlation analysis. Consequently, we had to exclude them from our correlation analysis. As a matter of fact, it is known that the proteins in these two cases undergo substantial conformational changes upon ligand binding. In the case of 1Q5L, global conformational changes occur, and dynamics of the β-domain are caused by peptide binding.[33] In the case of 2GTV, the protein structure is a loosely packed helix bundle and somehow demonstrates unprecedented flexibility at the millisecond time scale across its entire length.[35] Moreover, presteady-state kinetics data show that binding occurs by an induced fit mechanism on the same time scale as the enzymatic reaction. The present MM-PB/SA method assumes the similarity between the apo- and holo-form of the protein structure. If the apo-form is substantially different from the holo-form, then apparent discrepancy is expected in MM-PB/SA results.

Performance of Different Sampling Methods. As described in the Computational Methods Section, the standard way of the MM-PB/SA method is to average the binding free energies computed over a conformational ensemble of the given protein−ligand complex. Thus, different samplings of the possible conformations of the given complex may result in different outcomes. In fact, the original motivation of our study was to investigate the influence of different sampling methods on MM-PB/SA results. Comparing the statistical results in Tables 2 and 3, one can see that for both MM-PB/SA and MM-GB/SA, sampling method 2 produced notably better correlations between computed and experimental data ($R = 0.721$ and 0.788 for MM-PB/SA and MM-GB/SA, respectively, Figure 3) than the standard routine, i.e., method 1. This indicates that the results obtained on a single "representative" snapshot are statistically more accurate than those of the counterparts obtained by averaging over a conformational ensemble of the given protein−ligand complex.

We are not actually the first to come to this conclusion. For example, Stahl et al.[13] applied MM-PB/SA to three test sets regarding avidin (a set of 8 ligands) and p38 MAP (12 and 16 ligands in two sets, respectively). In their study, a conformational ensemble of 10 snapshots was selected for each complex from the resulting trajectory of a MD simulation of 200 ps long in explicit solvent. Based on their results, they stated that "applying the MM-PBSA energy function to a single, relaxed complex structure is an adequate and sometimes more accurate approach than the standard free energy averaging over molecular dynamics snapshots ..." Rastelli et al. also came to the same conclusion in their MM-PB/SA study of a set of 28 inhibitors of aldose reductase with experimentally determined crystal structures and inhibitory activities.[16] Although we come to basically the same conclusion, it should be mentioned that our results are based on conformational ensembles with experimental basis rather than computer-generated structural models. Due to the

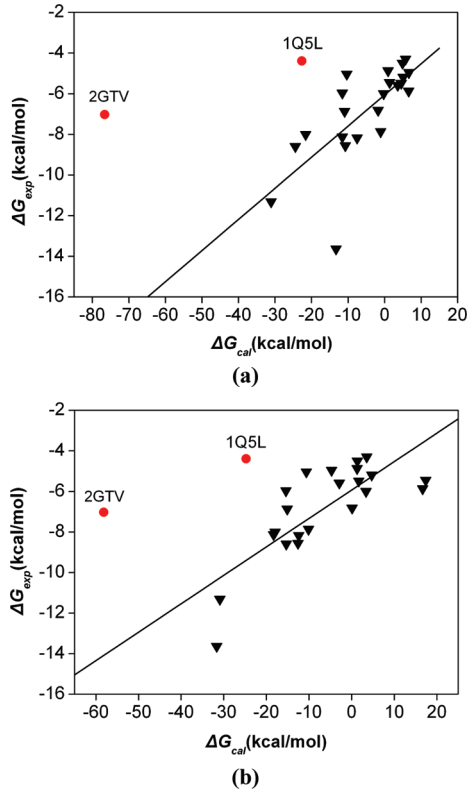

Figure 3. Correlations between the experimental binding free energies (ΔG_{exp}) and the calculated values (ΔG_{cal}) by considering only the "representative conformation" of each complex with (a) the MM-PB/SA method: $N = 22$, $R_p = 0.721$, SD = 1.63 kcal/mol and (b) the MM-GB/SA method: $N = 22$, $R_p = 0.788$, SD = 1.45 kcal/mol. PDB entries 1Q5L and 2GTV are not included in correlation analysis, which are indicated on this figure in red solid circles.

possible problems in current force fields and solvation models, quality of the computer-generated structural models is unpredictable. This is especially true on a diverse set of protein−ligand complexes. In contrast, our results are based on conformational ensembles with experimental basis. Thus, possible uncertainties introduced by defective computational methods are hopefully eliminated from our evaluation results.

Our results suggest that when applying the MM-PB/SA method to binding free energy calculation, one should rather focus on deriving the most reliable structures of the protein−ligand complexes under study. It is somewhat naïve to expect that averaging over a conformational ensemble will automatically give the right solution, needless to mention that it also requires extra computational costs. One may wonder why comparable or even better results can be obtained on a single representative structure rather than a conformational ensemble. According to the Boltzmann law, ensemble averages should be determined primarily by low-energy configurations. However, at the typical time scale of the MD simulations required by a MM-PB/SA application (0.5−10 ns), it is actually not certain if the molecular system under study reaches a true equilibrium state. Therefore, sampling the conformations on the resulting MD trajectory may or may not get meaningful ensemble averages. However, this is not the primary concern in our evaluation since the conformational ensembles considered by us are obtained through NMR measurements at a real time scale (minutes to hours). Thus, why averaging over a conformational ensemble is not a superior approach in MM-PB/SA computations has to be explained in other aspects. From a technical point of view, our MM-PB/SA and MM-GB/SA results exhibit fairly large fluctuations (up to ∼30 kcal/mol) on the given conformational ensembles of each complex. These large fluctuations mainly stem from the force field energy (E_{gas} in eq 3) and the electrostatic term in the solvation energy (G_{elec} in eq 4). Due to these unrealistic fluctuations in MM-PB/SA results, it is fairly unpredictable if the arithmetic averages across a conformational ensemble would effectively represent the true ensemble averages. For instead, MM-PB/SA computation based on a low-energy representative snapshot of the given complex is a shortcut to more reliable results.

How to choose a low-energy representative structure of a given protein−ligand complex, however, is a subtle issue. Our study, which relies on experimentally resolved structures to evaluate the MM-PB/SA method, does not intend to provide a direct answer to this question. The representative structures considered in our study are all given by the researchers who resolved those complex structures. It is reasonable to expect that they are selected by certain structural judgments (restraint violations and so on). However, the detailed methods for selecting such representative structures are not always clear in the original references. In practice, computational methods, such as MD simulations, are widely employed to the prediction of the three-dimensional structures of protein−ligand complexes when experimental methods are not applicable. In our study, another two sampling methods under test are also based on a single snapshot of the complex structure: Method 3 computes binding free energy using the conformation with the lowest force field energy among the conformational ensemble of each complex, while method 4 selects the lowest computed binding free energy among the conformational ensemble of each complex as the final prediction. Obviously, neither of them outperformed method 2 in both MM-PB/SA and MM-GB/SA results (Tables 2 and 3). In fact, they do not outperform the standard routine (method 1) either. Therefore, our results suggest that the meaningful "representative structure" of a given protein−ligand complex cannot be simply defined as the one with the lowest force field energy of the entire complex or the one with the lowest computed binding free energy between the complex. Our suggestion is that first of all, MD simulations of adequate length are necessary for obtaining structures close to a true equilibrium state. Then, some representative structures can be selected through cluster analysis on the resulting MD trajectory. These selected structures can be further evaluated by their energetic properties, and hopefully the most promising candidate can be identified among them.

In summary, our results suggest that it is actually more promising to conduct MM-PB/SA computation on a single representative structure rather than a conformational ensemble. This method produced more accurate results than the standard routine on the diverse set of protein−ligand complexes considered in our study. This method also has obvious technical advantages over the standard routine. For example, as discussed earlier in this article, including configurational entropy in MM-PB/SA or MM-GB/SA results produced better correlations between experimental and computed data. Nevertheless, computing configurational

Table 5. Correlations between the Experimental Binding Free Energies and the Binding Scores Computed by Four Scoring Functions[a]

	X-Score		PLP		DrugScore		ChemScore	
sampling methods	*R*	SD	*R*	SD	*R*	SD	*R*	SD
consider conformational ensembles (method 1)	0.646	1.80	0.636	1.82	0.559	1.96	0.421	2.14
consider the representative conformations (method 2)	0.677	1.74	0.653	1.79	0.564	1.95	0.610	1.87
consider the conformations with the lowest total energy (method 3)	0.626	1.84	0.718	1.64	0.567	1.94	0.432	2.13
consider the conformations with the best binding scores (method 4)	0.698	1.69	0.588	1.91	0.529	2.00	0.490	2.06

[a] All statistical results are computed based on the same 22 protein−ligand complexes used for evaluating MM-GB/SA and MM-PB/SA. *R* is the Pearson correlation coefficient, while SD is the standard deviation in linear fitting (in kcal/mol).

entropy requires a considerable amount of CPU time, which is clearly the most time-consuming step in the entire routine of MM-PB/SA. Computing this term for one conformation of a protein−ligand complex took two CPU hours on average on our workstation, while all other terms in eq 2 could be completed in one minute. Thus, reducing MM-PB/SA computation to one single structure will save a lot of computational costs. This practice will also avoid some other puzzles, such as the choice between the static or dynamic charge model.

Comparison with Scoring Functions. An interesting issue arises if MM-PB/SA computation is to be based on a single complex structure. In this way, MM-PB/SA is not much different from a scoring function. It can be considered as a force field-based function augmented with configurational entropy and a solvation energy terms. However, the CPU time for calculating a single complex structure by MM-PB/SA, typically in minutes, is slower approximately by 100-fold than current scoring functions applied in molecular docking. Considering that MM-PB/SA produces acceptable results on our test set, it is intriguing and also necessary to investigate if cheaper methods, like scoring functions, are able to provide results with comparable accuracy.

In our study, we performed a head-to-head comparison of the MM-PB/SA method with four selected scoring functions, including X-Score, PLP, ChemScore, and DrugScore, on the same test set used in our study. The statistical results produced by these scoring functions are summarized in Table 5. When computations are based on the representative conformations, X-Score and PLP produced correlation coefficients of 0.65−0.68, which are not much lower than the MM-PB/SA and MM-GB/SA results ($R = 0.72-0.79$). The results produced by DrugScore and ChemScore are somewhat less accurate ($R = 0.56-0.61$). In our study, all four scoring functions were also tested in combination with four different sampling methods. One can see in Table 5 that X-Score, PLP, and DrugScore are not very sensitive to different sampling methods. Since the representative conformations may not be straightforward to determine in practice, some robustness in this aspect is certainly a technical advantage. In contrast, the results of ChemScore are obviously inferior on conformational ensembles (method 1) than those obtained on single representative structures (method 2). The reason is not obvious since ChemScore as well as the other scoring functions was tested as black boxes in our study.

In summary, our results indicate that some selected scoring functions actually produce predictions close to MM-PB/SA or MM-GB/SA with much lower computational costs. In fact, we have found repeatedly that scoring functions are not necessarily less accurate than MM-PB/SA.[51] Note that a major point of our work presented here is that MM-PB/SA computations can be based on a single complex structure. This feature certainly makes MM-PB/SA a more practical choice for high-throughput jobs. Indeed, some researchers suggested[13] that the MM-PB/SA method can be applied as a postfilter in virtual screening to improve the chance of finding active compounds. Nevertheless, some appropriate docking/scoring schemes can fulfill this goal as well. The MM-PB/SA method, and perhaps other similar methods, would better be applied to study a particular set of protein−ligand complexes of interest after careful conformational sampling. Even for this type of study, scoring functions are also helpful since they can provide a reasonable estimation on whether the given set of binding data can be interpreted by computational methods.

CONCLUSION

We have evaluated the molecular mechanics Poisson−Boltzmann surface area (MM-PB/SA) method on a set of 24 diverse protein−ligand complexes. Our test set is unique in a way that each complex has a conformational ensemble derived from NMR spectroscopy. All previous evaluations of MM-PB/SA are based on computer-generated conformational ensembles, which may be associated with potential uncertainties introduced by defective computational methods. In contrast, our evaluation results should be least affected by this factor since they are obained on conformational ensembles with experimental basis. Consequently, the intrinsic quality of the MM-PB/SA method can be reflected more objectively.

Our results indicate that both MM-PB/SA and molecular mechanics generalized Born surface area (MM-GB/SA) are able to produce a modest correlation between their results and experimentally determined binding free energies on our test set. Considering that the MM-PB/SA method is typically applied to study a congeneric series of ligand molecules binding to an identical target protein, our study is probably the first to demonstrate that the MM-PB/SA method can also be applied successfully to a diverse set of protein−ligand complexes. However, both MM-PB/SA and MM-GB/SA failed to reproduce the absolute values of known binding free energies. They are thus more suitable for comparing the relative binding affinities of a group of protein−ligand

complexes. MM-GB/SA consistently produced more accurate and more converged results than those of MM-PB/SA on our test set, representing a more robust option for practical uses. Our results also demonstrate that inclusion of the configuration entropy helps to improve the final MM-PB/SA results. Nevertheless, MM-PB/SA and MM-GB/SA still tend to fail on protein−ligand complexes which undergo substantial conformational changes upon binding.

Another major finding of our study is that both MM-PB/SA and MM-GB/SA produced better results by considering a representative structure of each given complex (R = 0.72−0.79) than averaging the binding free energies over a conformational ensemble (R = 0.61−0.74). Thus, the preparative molecular dynamics simulations requried by MM-PB/SA should rather focus on finding a reliable structure of the given complex, and then this single structure can be used in subsequent MM-PB/SA computations. This routine is obviously more effective than the standard one. A head-to-head comparison of MM-PB/SA and MM-GB/SA with four selected scoring functions on the same test set reveals that MM-PB/SA and MM-GB/SA results are marginally better than those produced by the best scoring functions, supporting the value of the MM-PB/SA method. Scoring functions, however, are still more cost-effective options especially for high-throughput tasks.

ACKNOWLEDGMENT

The authors are grateful to the financial supports from the Chinese National Natural Science Foundation (Grants no. 20772149 and 90813006), the Chinese Ministry of Science and Technology (Grants no.2006AA02Z337 and 2009ZX09501-002), and the Science and Technology Commission of Shanghai Municipality (Grant no.074319113).

Supporting Information Available: The results produced by MM-PB/SA, MM-GB/SA, and four scoring functions on all 24 protein−ligand complexes considered in this study. This material is available free of charge via the Internet at http://pubs.acs.org.

REFERENCES AND NOTES

(1) Kollman, P. Free energy calculations: Applications to chemical and biochemical phenomena. *Chem. Rev.* **1993**, *93*, 2395–2417.
(2) Jorgensen, W. L. Free energy calculations: A breakthrough for modeling organic chemistry in solution. *Acc. Chem. Res.* **1989**, *22*, 184–189.
(3) Böhm, H. J.; Stahl, M. The use of scoring functions in drug discovery applications. In *Reviews in Computational Chemistry*; Lipkowitz, K. B., Boyd, D. B., Eds.; Wiley-VCH Inc.: Hoboken, NJ, 2002; Vol. 18, pp 41−88.
(4) Schulz-Gasch, T.; Stahl, M. Scoring functions for protein-ligand interactions: a critical perspective. *Drug Discovery Today: Tech.* **2004**, *1*, 231–239.
(5) Kollman, P. A.; Massova, I.; Reyes, C.; Kuhn, B.; Huo, S.; Chong, L.; Lee, M.; Lee, T.; Duan, Y.; Wang, W.; Donini, O.; Cieplak, P.; Srinivasan, J.; Case, D. A.; Cheatham, T. E. Calculating structures and free energies of complex molecules: Combining molecular mechanics and continuum models. *Acc. Chem. Res.* **2000**, *33*, 889–897.
(6) Kuhn, B.; Kollman, P. A. Binding of a diverse set of ligands to avidin and streptavidin: An accurate quantitative prediction of their relative affinity by a combination of molecular mechanics and continuum solvent models. *J. Med. Chem.* **2000**, *43*, 3786–3791.
(7) Lee, M. R.; Duan, Y.; Kollman, P. A. Use of MM-PB/SA in estimating the free energies of proteins: Application to native, intermediates, and unfolded villin headpiece. *Proteins: Struct., Funct., Genet.* **2000**, *39*, 309–316.
(8) Kasper, P.; Christen, P.; Gehring, H. Empirical calculations of the relative free energies of peptide binding to the molecular chaperone Dnak. *Proteins: Struct., Funct., Genet.* **2000**, *40*, 185–192.
(9) Xu, Y.; Wang, R. A computational analysis of the binding affinities of FKBP12 inhibitors using the MM-PB/SA method. *Proteins: Struct., Funct., Bioinf.* **2006**, *64*, 1058–1068.
(10) Brown, S. P.; Muchmore, S. W. High-throughput calculation of protein-ligand binding affinities: Modification and adaptation of the MM-PBSA protocol to enterprise grid computing. *J. Chem. Inf. Model.* **2006**, *46*, 999–1005.
(11) Steinbrecher, T.; Case, D. A.; Labahn, A. A multistep approach to structure-based drug design: Studying ligand binding at the human neutrophil elastase. *J. Med. Chem.* **2006**, *49*, 1837–1844.
(12) Brown, S. P.; Muchmore, S. W. Rapid estimation of relative protein-ligand binding affinities using a high-throughput version of MM-PBSA. *J. Chem. Inf. Model.* **2007**, *47*, 1493–1503.
(13) Kuhn, B.; Gerber, P.; Schulz-Gasch, T.; Stahl, M. Validation and use of the MM-PBSA approach for drug discovery. *J. Med. Chem.* **2005**, *48*, 4040–4048.
(14) Pearlman, D. A. Evaluating the molecular mechanics Poisson-Boltzmann surface area free energy method using a congeneric series of ligands to p38 MAP kinase. *J. Med. Chem.* **2005**, *48*, 7796–7807.
(15) Weis, A.; Katebzadeh, K.; Soderhjelm, P.; Nilsson, I.; Ryde, U. Ligand affinities predicted with the MM/PBSA method: Dependence on the simulation method and the force field. *J. Med. Chem.* **2006**, *49*, 6596–6606.
(16) Ferrari, A. M.; Degliesposti, G.; Sgobba, M.; Rastelli, G. Validation of an automated procedure for the prediction of relative free energies of binding on a set of aldose reductase inhibitors. *Bioorg. Chem. Med.* **2007**, *15*, 7865–7877.
(17) Berman, H. M.; Westbrook, J.; Feng, Z.; Gilliland, G.; Bhat, T. N.; Weissig, H.; Shindyalov, I. N.; Bourne, I. E. The Protein Data Bank. *Nucleic Acids Res.* **2000**, *28*, 235–242; http://www.rcsb.org/pdb/.
(18) Spronk, C.; Nabuurs, S. B.; Krieger, E.; Vriend, G.; Vuister, G. W. Validation of protein structures derived by NMR spectroscopy. *Prog. Nucl. Magn. Reson. Spectrosc.* **2004**, *45*, 315–337.
(19) Wang, R.; Fang, X.; Lu, Y.; Wang, S. The PDBbind database: Collection of binding affinities for protein-ligand complexes with known three-dimensional structures. *J. Med. Chem.* **2004**, *47*, 2977–2980.
(20) Wang, R.; Fang, X.; Lu, Y.; Yang, C. Y.; Wang, S. The PDBbind Database: Methodologies and updates. *J. Med. Chem.* **2005**, *48*, 4111–4119.
(21) Polshakov, V. I.; Birdsall, B.; Frenkiel, T. A.; Gargaro, A. R.; Feeney, J. Structure and dynamics in solution of the complex of *Lactobacillus casei* dihydrofolate reductase with the new lipophilic antifolate drug trimetrexate. *Protein Sci.* **1999**, *8*, 467–481.
(22) Zwahlen, C.; Li, S. C.; Kay, L. E.; Pawson, T.; Forman-Key, J. D. Multiple modes of peptide recognition by the PTB domain of the cell fate determinant Numb. *EMBO J.* **2000**, *19*, 1505–1515.
(23) Li, S. C.; Zwahlen, C.; Vincent, S. J. F.; McGlade, C. J.; Kay, L. E.; Pawson, T.; Forman-Key, J. D. Structure of a Numb PTB domain-peptide complex suggests a basis for diverse binding specificity. *Nat. Struct. Mol. Biol.* **1998**, *5*, 1075–1083.
(24) Sich, C.; Improta, S.; Cowley, D. J.; Guenet, C.; Merly, J.-P.; Teufel, M.; Saudek, V. Solution structure of a neurotrophic ligand bound to FKBP12 and its effects on protein dynamics. *Eur. J. Biochem.* **2000**, *267*, 5342–5354.
(25) Wang, P.; Beyon, L. I.-J.; Liao, H.; Beebe, K. D.; Yongkiettrakul, S.; Pei, D.; Tsai, M. D. II. Structure and specificity of the interaction between the FHA2 domain of rad53 and phosphotyrosyl peptides. *J. Mol. Biol.* **2000**, *302*, 927–940.
(26) Wang, X.; Li, M. X.; Spyracopoulos, L.; Beier, N.; Chandra, M.; Solaro, R. J.; Sykes, B. D. Structure of the C-domain of human cardiac troponin C in complex with the Ca2+ sensitizing drug EMD 57033. *J. Biol. Chem.* **2001**, *276*, 25456–25466.
(27) Wang, X.; Li, M. X.; Sykes, B. D. Structure of the regulatory N-domain of human cardiac troponin C in complex with human cardiac troponin I147−163 and bepridil. *J. Biol. Chem.* **2002**, *277*, 31124–31133.
(28) Urbaniak, M. D.; Muskett, F. W.; Finucane, M. D.; Caddick, S.; Woolfson, D. N. Solution structure of a novel chromoprotein derived from apo-neocarzinostatin and a synthetic chromophore. *Biochemistry* **2002**, *41*, 11731–11739.
(29) Takashima, H.; Yoshida, T.; Ishino, T.; Hasuda, K.; Ohkubo, T.; Kobayashi, Y. Solution NMR structure investigation for releasing mechanism of neocarzinostatin chromophore from the holoprotein. *J. Biol. Chem.* **2005**, *280*, 11340–11346.
(30) Pires, J. R.; Taha-Nejad, F.; Toepert, F.; Ast, T.; Hoffmuller, U.; Schneider-Mergener, J.; Kuhne, R.; Macias, M. J.; Oschkinat, H. Solution structures of the YAP65 WW domain and the variant L30K in complex with the peptides GTPPPPYTVG, N-(n-octyl)-GPPPY and PLPPY and the application of peptide libraries reveal a minimal binding epitope. *J. Mol. Biol.* **2001**, *314*, 1147–1156.

(31) Freund, C.; Kuhne, R.; Yang, H. L.; Park, S.; Reinherz, E. L.; Wagner, G. Dynamic interaction of CD2 with the GYF and the SH3 domain of compartmentalized effector molecules. *EMBO. J.* **2002**, *21*, 5985–5995.

(32) Cao, C.; Kwon, K.; Jiang, Y. L.; Drohat, A. C.; Stivers, J. T. Solution structure and base perturbation studies reveal a novel mode of alkylated base recognition by 3-methyladenine DNA glycosylase I. *J. Biol. Chem.* **2003**, *278*, 48012–48020.

(33) Stevens, S. Y.; Cai, S.; Pellecchia, M.; Zuiderweg, E. R. P. The solution structure of the bacterial HSP70 chaperone protein domain DnaK(393−507) in complex with the peptide NRLLLTG. *Protein Sci.* **2003**, *12*, 2588–2596.

(34) Swarbrick, J. D.; Buyya, S.; Gunawardana, D.; Gayler, K. R.; McLennan, A. G.; Gooley, P. R. Structure and substrate-binding mechanism of human Ap4A hydrolase. *J. Biol. Chem.* **2005**, *280*, 8471–8481.

(35) Pervushin, K.; Vamvaca, K.; Vogeli, B.; Hilvert, D. Structure and dynamics of a molten globular enzyme. *Nat. Struct. Mol. Biol.* **2007**, *14*, 1202–1206.

(36) Taverna, S. D.; Ilin, S.; Rogers, R. S.; Tanny, J. C.; Lavender, H.; Li, H.; Baker, L.; Boyle, J.; Blair, L. P.; Chait, B. T.; Patel, D. J.; Aitchison, J. D.; Tackett, A. J.; Allis, C. D. Yng1 PHD finger binding to H3 trimethylated at K4 promotes NuA3 HAT activity at K14 of H3 and transcription at a subset of targeted ORFs. *Mol. Cell* **2006**, *24*, 785–796.

(37) Runyon, S. T.; Zhang, Y.; Appleton, B. A.; Sazinsky, S. L.; Wu, P.; Pan, B.; Wiesmann, C.; Skelton, N. J.; Sidhu, S. S. Structural and functional analysis of the PDZ domains of human HtrA1 and HtrA3. *Protein Sci.* **2007**, *16*, 2454–2471.

(38) Ramirez-Espain, X.; Ruiz, L.; Martin-Malpartida, P.; Oschkinat, H.; Macias, M. J. Structural characterization of a new binding motif and a novel binding mode in group 2 WW domains. *J. Mol. Biol.* **2007**, *373*, 1255–1268.

(39) Liu, Y.; Henry, G. D.; Hegde, R. S.; Baleja, J. D. Solution structure of the hDlg/SAP97 PDZ2 domain and its mechanism of interaction with HPV-18 Papillomavirus E6 protein. *Biochemistry* **2007**, *46*, 10864–10874.

(40) Mansy, S. S.; Zhang, J.; Kummerle, R.; Nilsson, M.; Chou, J. J.; Szostak, J. W.; Chaput, J. C. Structure and evolutionary analysis of a non-biological ATP-binding protein. *J. Mol. Biol.* **2007**, *371*, 501–513.

(41) Case, D. A.; Darden, T. A.; Cheatham, T. E.; Simmerling, C. L.; Wang, J.; Duke, R. E.; Luo, R.; Merz, K. M.; Pearlman, D. A.; Crowley, M.; Walker, R. C.; Zhang, W.; Wang, B.; Hayik, S.; Roitberg, A.; Seabra, G.; Wong, K. F.; Paesani, F.; Wu, X.; Brozell, S.; Tsui, V.; Gohlke, H.; Yang, L.; Tan, C.; Mongan, J.; Hornak, V.; Cui, G.; Beroza, P.; Mathews, D. H.; Schafmeister, C.; Ross, W. S.; Kollman, P. A. *AMBER 9*; University of California: San Francisco, CA, 2006.

(42) Frisch, M. J. Trucks, G. W.; Schlegel, H. B.; Scuseria, G. E.; Robb, M. A.; Cheeseman, J. R.; Montgomery, Jr., J. A.; Vreven, T.; Kudin, K. N.; Burant, J. C.; Millam, J. M.; Iyengar, S. S.; Tomasi, J.; Barone, V.; Mennucci, B.; Cossi, M.; Scalmani, G.; Rega, N.; Petersson, G. A.; Nakatsuji, H.; Hada, M.; Ehara, M.; Toyota, K.; Fukuda, R.; Hasegawa, J.; Ishida, M.; Nakajima, T.; Honda, Y.; Kitao, O.; Nakai, H.; Klene, M.; Li, X.; Knox, J. E.; Hratchian, H. P.; Cross, J. B.; Bakken, V.; Adamo, C.; Jaramillo, J.; Gomperts, R.; Stratmann, R. E.; Yazyev, O.; Austin, A. J.; Cammi, R.; Pomelli, C.; Ochterski, J. W.; Ayala, P. Y.; Morokuma, K.; Voth, G. A.; Salvador, P.; Dannenberg, J. J.; Zakrzewski, V. G.; Dapprich, S.; Daniels, A. D.; Strain, M. C.; Farkas, O.; Malick, D. K.; Rabuck, A. D.; Raghavachari, K.; Foresman, J. B.; Ortiz, J. V.; Cui, Q.; Baboul, A. G.; Clifford, S.; Cioslowski, J.; Stefanov, B. B.; Liu, G.; Liashenko, A.; Piskorz, P.; Komaromi, I.; Martin, R. L.; Fox, D. J.; Keith, T.; Al-Laham, M. A.; Peng, C. Y.; Nanayakkara, A.; Challacombe, M.; Gill, P. M. W.; Johnson, B.; Chen, W.; Wong, M. W.; Gonzalez, C.; and Pople, J. A. *Gaussian 03*, revision C.02; Gaussian, Inc.: Wallingford, CT, 2004.

(43) Bayly, C. I.; Cieplak, P.; Cornell, W.; Kollman, P. A. A well-behaved electrostatic potential based method using charge restraints for deriving atomic charges: the RESP model. *J. Phys. Chem.* **1993**, *97*, 10269–10280.

(44) Wang, R.; Lai, L.; Wang, S. Further development and validation of empirical scoring functions for structure-based binding affinity prediction. *J. Comput.-Aided Mol. Des.* **2002**, *16*, 11–26.

(45) Velec, H. F. G.; Gohlke, H.; Klebe, G. DrugScore(CSD): Knowledge-based scoring function derived from small molecule crystal data with superior recognition rate of near-native ligand poses and better affinity prediction. *J. Med. Chem.* **2005**, *48*, 6296–6303.

(46) Verkhivker, G.; Appelt, K.; Freer, S. T.; Villafranca, J. E. Empirical free energy calculations of ligand-protein crystallographic complexes. I. Knowledge-based ligand-protein interaction potentials applied to the prediction of human immunodeficiency virus 1 protease binding affinity. *Protein Eng.* **1995**, *8*, 677–691.

(47) Verkhivker, G. M.; Bouzida, D.; Gehlhaar, D. K.; Rejto, P. A.; Arthurs, S.; Rose, P. W. Deciphering common failures in molecular docking of ligand-protein complexes. *J. Comput.-Aided Mol. Des.* **2000**, *14*, 731–751.

(48) Eldridge, M. D.; Murray, C. W.; Auton, T. R.; Paolini, G. V.; Mee, R. P. Empirical scoring functions: I. The development of a fast empirical scoring function to estimate the binding affinity of ligands in receptor complexes. *J. Comput.-Aided Mol. Des.* **1997**, *11*, 425–445.

(49) Murray, C. W.; Auton, T. R.; Eldridge, M. D. Empirical scoring functions. II. The testing of an empirical scoring function for the prediction of ligand-receptor binding affinities and the use of Bayesian regression to improve the quality of the model. *J. Comput.-Aided Mol. Des.* **1998**, *12*, 503–519.

(50) Cheng, T.; Li, X.; Li, Y.; Liu, Z.; Wang, R. Comparative assessment of scoring functions on a diverse test set. *J. Chem. Inf. Model.* **2009**, *49*, 1079–1093.

(51) Zhang, X.; Li, X.; Wang, R. Interpretation of the binding affinities of PTP1B inhibitors with the MM-GB/SA method and the X-Score scoring function. *J. Chem. Inf. Model.* **2009**, *49*, 1033–1048.

(52) Lamm, G. In *Reviews in Computational Chemistry*; Lipkowitz, K. B., Larter, R., Cundari, T. R., Eds; John Wiley & Sons Inc.: Hoboken, NJ, 2003; Vol. 19, pp147−365.

(53) Baker, N. A. In *Reviews in Computational Chemistry*; Lipkowitz, K. B., Larter, R., Cundari, T. R., Eds; John Wiley & Sons Inc.: Hoboken, NJ, 2005; Vol. 21, pp349−379.

(54) Bashford, D.; Case, D. A. Generalized Born Models of Macromolecular Solvation Effects. *Annu. Rev. Phys. Chem.* **2000**, *51*, 129–152.

(55) Still, W. C.; Tempczyk, A.; Hawley, R. C.; Hendrickson, T. Semianalytical treatment of solvation for molecular mechanics and dynamics. *J. Am. Chem. Soc.* **1990**, *112*, 6127–6129.

(56) Wang, J.; Morin, P.; Wang, W.; Kollman, P. A. Use of MM-PBSA in reproducing the binding free energies to HIV-1 RT of TIBO derivatives and predicting the binding mode to HIV-1 RT of Efavirenz by docking and MM-PBSA. *J. Am. Chem. Soc.* **2001**, *123*, 5221–5230.

(57) Xiong, Y.; Li, Y.; He, H.; Zhan, C. Theoretical calculation of the binding free energies for pyruvate dehydrogenase E1 binding with ligands. *Bioorg. Med. Chem. Lett.* **2007**, *17*, 5186–5190.

(58) Khoruzhii, O.; Donchev, A. G.; Galkin, N.; Illarionov, A.; Olevanov, M.; Ozrin, V.; Queen, C.; Tarasov, V. Application of a polarizable force field to calculations of relative protein-ligand affinities. *Proc. Natl. Acad. Sci. U.S.A.* **2008**, *105*, 10378–10383.

CI100036A